1 July 2002

Optics Communications 208 (2002) 191–196

OPTICS COMMUNICATIONS

www.elsevier.com/locate/optcom

Phase analysis of nonlinear femtosecond pulse propagation and self-frequency shift in optical fibers

Fiorenzo G. Omenetto[a,*], Yeojin Chung[b], Dzmitry Yarotski[c], Tobias Schaefer[c], Ildar Gabitov[c], Antoinette J. Taylor[a]

[a] *Materials Science and Technology Division, MST-10, MSK764, Los Alamos National Laboratory, Los Alamos, NM 87545, USA*
[b] *Department of Mathematics, University of California Irvine, Irvine, CA 92697-5255, USA*
[c] *Theoretical Division, T-7, Los Alamos National Laboratory, Los Alamos, NM 87545, USA*

Received 30 October 2001; received in revised form 9 April 2002; accepted 17 April 2002

Abstract

Phase sensitive analysis of femtosecond pulse propagation in optical fibers employing frequency resolved optical gating (FROG) is presented and compared to numerical simulations employing a modified cubic nonlinear Schrödinger equation (NLSE). Phase information obtained from deconvolution of the experimental traces allows the observation and characterization of specific pulse propagation features as a function of energy and distance. The experimental observation of the phase signature of a soliton during propagation and the phase properties of the soliton self-frequency shift are described and are found to be in remarkable agreement with the simulations. © 2002 Elsevier Science B.V. All rights reserved.

1. Introduction

Recent progress in telecommunications systems has led to increasing development and use of ultrafast technologies [1]. Understanding the evolution of pulses on the femtosecond scale is a challenging task, since dispersive effects and nonlinearities become dominant factors. At the onset of the nonlinear pulse propagation regime, which occurs generally on the picosecond timescale, a balance between chromatic dispersion and nonlinear effects (in the anomalous dispersion regime) leads to the formation of optical solitons. These are of particular appeal due to their potential applications in telecommunications [2]. When pulsewidths are decreased to the femtosecond regime and input pulse powers are increased, however, higher order dispersion and nonlinearity complicate the dynamics of ultrashort pulse propagation. Chirp on the initial pulse, furthermore, affects these dynamics and the balance between linear and nonlinear effects becomes affected by a multitude of competing phenomena. Access to the temporal and spectral phase information of propagating femtosecond pulses, in addition to their spectral and temporal features, provides an effective mean to probe these nonlinear processes. Understanding

* Corresponding author. Tel.: +1-505-665-5847; fax: +1-505-665-7652.
E-mail address: omenetto@lanl.gov (F.G. Omenetto).

0030-4018/02/$ - see front matter
PII: S0030-4018(02)01496-7

the latter would clarify various issues such as the delivery of ultrashort pulses through fibers for medical applications and imaging [3], supercontinuum recompression and control from highly nonlinear photonic crystal fibers [4,5], and coherent control in optical fibers [6], as well as the design and implementation of the next generation of telecommunications systems. An increasing interest in the measurement of the electric field contained within the propagating optical pulse envelope by using various phase sensitive detection techniques [7–9] has developed recently. Detailed analysis of the dynamics of pulse propagation has also been performed with the help of these techniques [2,7].

In the present work, we extend this approach to address longer lengths of fiber and higher input pulse powers with particular attention to the phase features and dynamics of the pulses during propagation. Experimental results illustrating the propagation of a fundamental soliton throughout a $\sim$100 m optical fiber are presented. We add to these results, for the first time to our knowledge, the experimentally observed temporal phase features of the pulses during soliton propagation, that is shown to be consistently flat across the pulse in different positions along the fiber link. Analysis of the pulse phase features for increasing power values is also performed. In this regime, the pulse is subject to the well known self-frequency shift. Through phase sensitive techniques, the nature and evolution of the electric field's temporal phase is experimentally analyzed for the first time revealing that *only under certain propagation conditions* the self-shifted pulse actually assumes the features of a soliton, undergoing amplitude and temporal oscillations reminiscent of chirped pulse propagation [10]. The experimental results are compared with modeling using a modified nonlinear Schrödinger code, obtaining excellent agreement and validation of the numerical approach employed.

2. Experimental results

Phase-sensitive detection is obtained by using a single-shot frequency resolved optical gating (FROG) arrangement [11] previously described for studies of femtosecond pulse propagation in the near-infrared. With this arrangement, we previously reported on the phase dynamics of soliton formation in a 10 m link of conventional single-mode fiber, detecting features such as the characteristic oscillations that occur as a chirped pulse evolves into a soliton [2].

The experimental approach is briefly outlined as follows: pulses having duration $\tau \sim 170$ fs generated by an optical parametric oscillator tuned to $\lambda = 1.55$ μm ($E = 3.5$ nJ at 80 MHz) are attenuated and coupled into a link of single-mode optical fiber (Corning SMF-28). These pulses exhibit a slight linear chirp. The output from the fiber is sent to a single-shot SHG-FROG arrangement. Pulse propagation through the fiber can be examined and followed with the cutback method. The pulse energies are carefully varied before being launched into a fixed-length segment of fiber and FROG traces are correspondingly detected. The fiber is then cut and the process repeated allowing both fixed-length energy-dependent measurements as well as propagation studies at fixed pulse energies. A particularly illuminating case to illustrate phase-sensitive analysis is obtained by observing the pulse propagation in the soliton regime (Fig. 1). Under analogous experimental conditions, previous measurements [2] have indicated a range of input pulse energies of 270 ± 10 pJ for the onset of soliton formation. The pulses that are sent through the 90 m fiber link have an energy of 280 pJ, and FROG traces are taken for different fiber lengths to follow pulse propagation. After deconvolution of the traces it can be noted that the phase is noticeably flat across the pulse during propagation indicating temporal phase coherence, which is a signature of a soliton traveling through the fiber.

As the input pulse power is increased, oscillations in the pulsewidth appear, consistent with those observed at lower powers corresponding to chirped pulse dynamics leading to soliton formation [2]. Analogous oscillations occur in the pulsewidth as the Raman-induced self-frequency shift causes the carrier wavelength to vary as it travels through the optical fiber. Modeling femtosecond pulse propagation becomes a harder task that has to account for the concurrent effects of

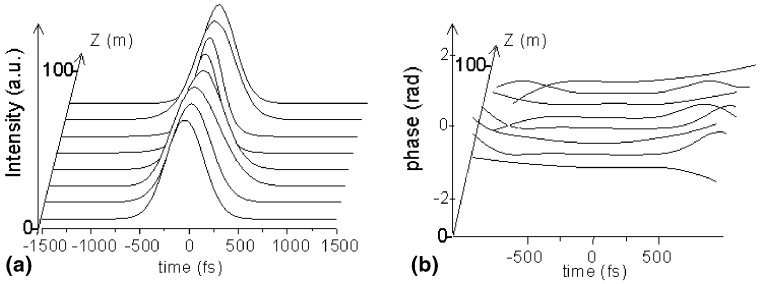

Fig. 1. Experimental data illustrating the propagation of a soliton. The graph shows (a) reconstructed electric field and (b) temporal phase profiles for a $t = 170$ fs, $E = 270$ pJ pulse propagating in a 90 m fiber link of conventional single-mode optical fiber. The spatial slices are separated by 10 m. The temporal phase profiles of the individual pulses in (b) have been shifted by a constant to realize the graph.

shifting, and temporal and amplitude variations. As femtosecond pulses propagate in a fiber, phonon modes of amorphous silica are excited locally and instantaneously, mediating the transfer of energy from the higher to the lower frequency components of the pulse and influencing the Raman line shape. Under these conditions, modeling the propagation becomes more complex [12]. Along these lines, the time delayed Raman response becomes important. Therefore, to compare the numerical simulation to the experimental data, we have included higher order corrections in the nonlinear Schrödinger equation. Besides modeling the temporal evolution of the pulse, the time-dependent phase behavior of the electric field is also calculated and compared to experimental data obtained by reconstruction of the FROG traces. The self-frequency shift of the pulse is also included in the calculations and compared to the experimentally observed Raman shift.

The model used to describe the pulse propagation is based on the commonly employed lossless nonlinear Schrödinger equation (NLSE) $\partial A/\partial Z + \mathrm{i}/2\beta_2\partial^2 A/\partial T^2 = \mathrm{i}\gamma|A|^2 A$. In the femtosecond regime, one must take into account higher order dispersion due to the bandwidth of femtosecond pulses and intensity dependent terms such as the delayed Raman response. With the addition of fiber loss the equation becomes

$$\partial A/\partial Z + \alpha/2A + \mathrm{i}/2\beta_2\partial^2 A/\partial T^2 - 1/6\beta_3\partial^3 A/\partial T^3 = \mathrm{i}\gamma(|A|^2 A - T_\mathrm{R} A\partial|A|^2/\partial T), \quad (1)$$

where A represents the pulse envelope, Z is the distance in km, T is the time in femtoseconds, α is the loss coefficient, β_2 and β_3 represent the second- and third-order dispersions, γ represents the nonlinear term and T_R is the time delayed Raman response.

To associate the derived equation to the physical conditions of the experiment, we further transform Eq. (1) to a dimensionless equation and use as input parameters to the modified equation the values of pulsewidth and chirp obtained experimentally from the reconstructed FROG traces of the input pulses at various powers. The characteristic distances for dispersion, nonlinear effects and losses provide a measure of the distance it takes for these effects to influence pulse propagation. The parameters used in the calculations are obtained from the published values for Corning SMF-28 ($\beta_{2,3}$ as a function of wavelength is calculated using $D = 0.023/4(\lambda - \lambda_0^4/\lambda^3)$ ps/nm km, $A_\mathrm{eff} = 80$ μm^2 at 1.55 μm and $n_2 = 3 \times 10^{-20}$ m^2/W). These quantities are defined as [13] $Z_\mathrm{Disp2} = 2T_\mathrm{FWHM}^2/\beta_2$, $Z_\mathrm{Disp3} = 6T_\mathrm{FWHM}^3/\beta_3$, $Z_\mathrm{NL} = 1/(\gamma P_\mathrm{peak})$, and $Z_\mathrm{Loss} = 2/\alpha$. In our case, for an initial pulse having a duration of 170 fs, and an average power of 45 mW, the characteristic parameters are $Z_\mathrm{Disp2} = 2.83 \times 10^{-3}$ km, $Z_\mathrm{Disp3} = 2.86 \times 10^{-2}$ km, $Z_\mathrm{NL} = 2.95 \times 10^{-3}$ km, $Z_\mathrm{Loss} = 22.86$ km, accounting for the scaling of the effective area with wavelength. The experimental results of the characterization of the propagation of the pulse and the comparison with the NLSE calculations are illustrated in Figs. 2 and 3. Fig. 2(a) shows the

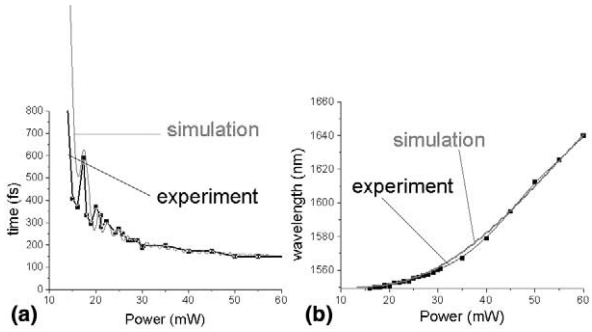

Fig. 2. Comparison of experimental data and numerical calculations for (a) pulsewidth variation as a function of power and (b) Raman self-frequency shift for a $t = 170$ fs pulse propagating through $Z = 40$ m of single mode fiber. The data points are indicated by squares in the graph. The simulation results track the experimental data in both cases.

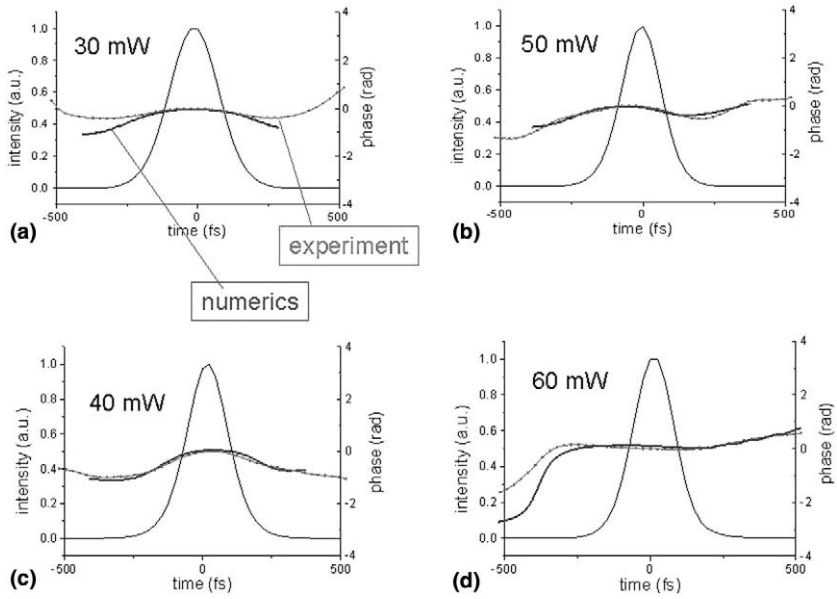

Fig. 3. Experimental intensity and phase profiles obtained from deconvolution of the FROG traces at the output of a $Z = 40$ m segment of single mode fiber for increasing power. In the plots, the numerically calculated phase functions obtained from the NLSE simulations are also plotted. The latter, which are shifted by a constant phase factor k to better compare with the experimentally obtained data, faithfully reproduce the phase dynamics one over the central portion of the pulse. The flat phase observed for the $P = 60$ MW case is indicative of temporal coherence typical of a self-frequency shifted soliton.

evolution of the pulse duration for increasing power and the Raman shift in a fixed segment of fiber having a length of $Z = 40$ m. As expected, the initial chirp of the input induces oscillations as the pulse duration shortens.

Whereas simplistic dispersive wave propagation can be argued to be the dominant cause of the oscillations, Nishizawa et al. [14] have shown that there is a much more complex interplay given the frequency dependence of a number of parameters (such as the nonlinear coefficient, the effective area/mode size, and certainly the dispersion curve characteristics). Furthermore, the initial chirp of the pulse plays a critical role in determining the

oscillation frequencies of the pulse as it evolves towards a soliton [10].

The experimentally detected pulsewidth dynamics are in excellent agreement with the numerical predictions. Fig. 2(b) shows the comparison between the calculated and the experimental self-frequency shift. In this case the maximum shift detected for the $Z = 40$ m link of conventional SMF-28 fiber, with no polarization control, is of the order of 100 nm. Theoretical and experimental findings indicate that there is proportionality between Δv and the square of the average power P^2 (i.e. $\Delta v \propto \tau^{-4}$) [14–16]. This relationship is indeed verified for the range of energies illustrated here.

The interaction of a soliton with dispersive waves was more realistically modeled by Kuztnesov et al. [17], describing the oscillatory nature of pulse propagation due to the interplay of the soliton with the dispersive waves. This paper described oscillations in an integrable case, whereas our experiments operate in a non-integrable NLSE regime where agreement between model and experiment should be more difficult. Further confirmation of the validity of the model is achieved by comparison of the calculated temporal phase function with the experimentally recovered phase function through FROG. The results of these simulations, along with the experimental data, are shown in Fig. 3. In this case, a comparison is performed between the experimentally observed phases and the calculated ones for increasing pulse power in the $Z = 40$ m case. Again, the experimental results and the calculated ones are in good agreement, which is especially notable given that the pulse is undergoing a spectral shift in addition to experiencing temporal oscillations. The modified NLSE is capable of tracking the phase variation while the Raman effect is causing the pulse to self-frequency shift. The phase functions indicate that at a particular instant (Fig. 3(d)) a near-flat phase is observed across the center of the pulse thus confirming the formation of a temporal soliton. At lower energies the pulse eventually settles to the predicted asymptotic soliton waveform [2,18]. At these high intensities, however, the continuous frequency shift makes the dynamics more complex, and the flat temporal phase, signature of a soliton, is observed only for a given combination of frequency shift and pulse energy.

Validation of the model through the experiment confirms applicability of the NLSE to accurately model femtosecond pulse propagation in optical fibers while the Raman (and other) effect is acting upon the pulse. We believe this to be a non-trivial result, given the agreement between theory and experiment.

In summary, the phase details, obtained through reconstruction of the FROG traces, have allowed the observation of a stable flat phase during propagation of a soliton through a 90 m fiber link and have enabled the identification amidst temporal breathing and Raman-shifting of the propagating pulse, a self-frequency shifted soliton. The experimental observations are backed by NLSE calculations that describe the frequency dependent (amplitude and phase) pulse dynamics in these experiments. Application of this joint theoretical and experimental methodologies constitutes an effective tool for the understanding of physical mechanisms that govern nonlinear pulse propagation in optical fibers.

Acknowledgements

This research was supported by the Los Alamos Directed Research and Development Program of the US Department of Energy and by (IG) DOE contract W-7-405-ENG-36 and by the DOE program in Applied Mathematical Sciences, KI-01-01. F.G.O. acknowledges the Los Alamos Office of the Director for the support received with the J. Robert Oppenheimer fellowship.

References

[1] W.H. Knox, IEEE JSTQE 6 (6) (2000) 1273.
[2] F.G. Omenetto, B. Luce, D. Yarotski, A.J. Taylor, Opt. Lett. 24 (1999) 1392.
[3] E.B. Brown, E. Wu, W. Zipfel, W.W. Webb, Biophys. J. 77 (5) (1999) 1835.
[4] M.W. Kimmel, R. Trebino, J. Ranka, A.J. Stentz., CLEO 2000, CFL7, San Francisco.
[5] J.C. Knight et al., Science 282 (1998) 1476.
[6] F.G. Omenetto et al., Opt. Lett. 26 (12) (2001) 938.

[7] J.M. Dudley, L.P. Barry, P.G. Bollond, J.D. Harvey, R. Leonhardt, P.D. Drummond, Opt. Lett. 22 (1997) 457.
[8] N. Nishizawa, T. Goto, Opt. Express 8 (6) (2001) 328.
[9] K. Taira, K. Kikuchi, Electron. Lett. 37 (5) (2001) 311.
[10] C. Desem, P.L. Chu, Opt. Lett. 11 (4) (1986) 248.
[11] F.G. Omenetto, J.W. Nicholson, A.J. Taylor, Opt. Lett. 24 (23) (1999) 1780.
[12] G. Falkovsky, Phys. Rev. B 64 (2001) 24301.
[13] G. Agrawal, Nonlinear Fiber Optics, Academic Press, Orlando, FL, 1989.
[14] N. Nishizawa et al., Jpn. J. Appl. Phys. 38 (8) (1999) 4768.
[15] F.M. Mitschke, L.F. Mollenauer, Opt. Lett. 11 (10) (1986) 659.
[16] J.P. Gordon, Opt. Lett. 11 (10) (1986) 663.
[17] E. Kuztnesov et al., Physica D 87 (1995) 201.
[18] D.J. Kane, R. Trebino, IEEE J. Quantum Electron. 29 (2) (1993) 571.